1-1-2008

Nonlinear analysis and behavior of concrete-filled steel tubular beam-columns

Qing Quan Liang
University of Southern Queensland

Muhammad N. S Hadi
University of Wollongong, mhadi@uow.edu.au

Nonlinear Analysis and Behavior of Concrete-Filled Steel Tubular Beam-Columns

Qing Quan Liang
Faculty of Engineering and Surveying, University of Southern Queensland, Toowoomba, QLD 4350, Australia

Muhammad N. S. Hadi
School of Civil, Mining and Environmental Engineering, University of Wollongong, Wollongong, NSW 2522, Australia

ABSTRACT: This paper presents a nonlinear fiber element analysis method for predicting the behavior of short concrete-filled steel tubular (CFST) beam-columns under axial load and biaxial bending. Nonlinear constitutive models for confined concrete and structural steel are considered in the fiber element analysis. Efficient secant algorithms are developed to iterate the depth and orientation of the neutral axis within the composite section to satisfy equilibrium conditions. The accuracy of the fiber element method is established by comparisons with existing solutions. The fiber element analysis program developed is employed to study the effects of steel ratios and concrete strengths on the axial load-bending moment interaction curves for CFST beam-columns. The proposed fiber element analysis technique is shown to be efficient and can be used directly in the design of CFST beam-columns.

1 INTRODUCTION

Concrete-filled steel tubular columns are efficient structural members, which possess high structural performance in terms of strength, ductility and strain energy absorption capacity. High strength concrete is increasingly used in CFST columns in high rise construction. The analysis of high strength CFST beam-columns under axial load and biaxial bending is complex and current design codes do not provide sufficient specifications for the design of such columns. Experiments can be conducted to investigate the inelastic behavior of CFST beam-columns and to verify numerical methods, but they are expensive and time-consuming. These highlight the need for an advanced computational technique for the nonlinear analysis and design of CFST beam-columns.

Experiments on the ultimate load behavior of CFST columns have been conducted by many researchers (Furlong 1967; Knowles and Park 1969; Shakir-Khalil and Mouli 1990; Schneider 1998). Tests on thin-walled CFST columns under axial compression indicated that the local buckling behavior of the steel box is characterized by the outward buckling mode that increases its local buckling resistance when compared to a hollow steel box (Ge and Usami 1992; Bridge et al. 1995; Uy 1998, 2000). Theoretical studies on local buckling of steel plates in thin-walled composite members have been undertaken by Wright (1995), Liang and Uy (2000) and Liang et al. (2004, 2007).

Nonlinear analysis methods for predicting the behavior of composite columns have been developed (Spacone and El-Tawil 2004). El-Tawil et al. (1995) and El-Tawil and Deierlein (1999) proposed a fiber element method for the nonlinear analysis of concrete-encased composite columns under axial load and biaxial bending. Hajjar and Gourley (1996) employed fiber element analysis to generate strength interaction diagrams for CFST beam-columns. Lakshmi and Shanmugam (2002) presented a semi-analytical model for determining the ultimate load behavior of concrete-filled steel box columns. Their model does not consider the effects of concrete confinement and concrete tensile strength. Mursi and Uy (2003) presented an analytical method for the nonlinear analysis of CFST columns under uniaxial bending. Liang et al. (2006) developed a fiber element analysis technique for the nonlinear analysis of axially loaded thin-walled CFST columns with local buckling effects.

In this paper, a nonlinear fiber element analysis method is developed for predicting the ultimate strengths of CFST columns under axial load and biaxial bending. The concrete confinement effect is considered in the concrete model. Efficient secant algorithms are developed to iterate the depth and orientation of the neutral axis in the composite section to satisfy equilibrium conditions. The fiber element analysis technique is validated by existing solutions. The effects of steel ratios and concrete strengths on the axial load-bending moment interaction curves for

CFST columns are investigated by using the fiber element analysis technique. The method of analysis presented can be applied to CFST columns under uniaxial and biaxial bending.

2 FIBER ELEMENT ANALYSIS

2.1 *Fiber element discretization*

The fiber element analysis is a numerical method for determining the strength and stiffness of member cross sections (El-Tawil and Deierlein 1999). In the fiber element method, the composite section is discretized into many small regions (fiber elements), as shown in Figure 1. Each element represents a fiber of material running longitudinally along the member. Constitutive models are based on the uniaxial stress-strain relationships of materials. Stress resultants are obtained by numerical integration of stresses through the composite cross section.

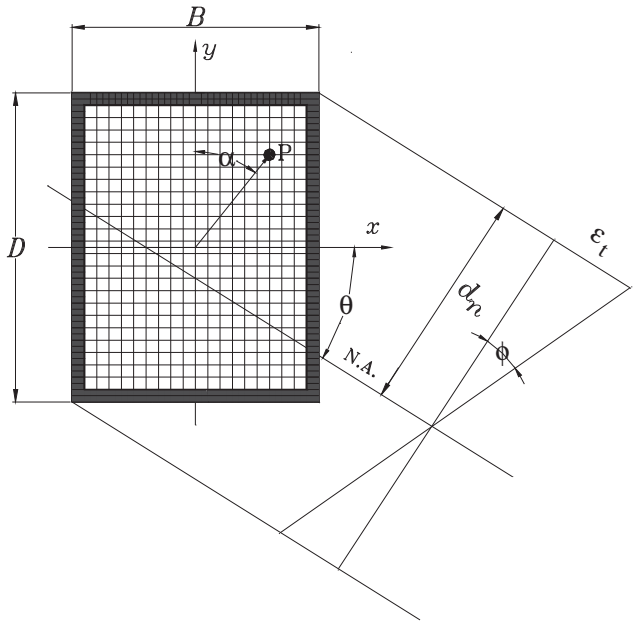

Figure 1. Cross-section of CFST column under axial load and biaxial bending

2.2 *Assumptions*

The proposed fiber element analysis method is based on the following assumptions:

(1) Plane sections remain plane after deformation, resulting in linear distribution of strain.
(2) The effects of strain hardening, residual stresses and local buckling of steel plates are not considered.
(3) Failure occurs when the strain of the extreme compression fiber of concrete reaches the maximum strain.
(4) The effect of concrete confinement on the ductility is considered.
(5) Tensile strength of concrete is considered.

2.3 *Material stress-strain relationships*

In the present fiber element method, the idealized elastic to perfectly plastic stress-strain relationship was used for structural steel. The strain hardening of steel was not considered.

It is assumed that the confinement effect increases only the ductility of the encased concrete in a concrete-filled steel box column but not its ultimate strength as suggested by Tomii and Sakino (1979). The general stress-strain curve for concrete in concrete-filled steel box columns is depicted in Figure 2. The part OA of the stress-strain curve is modeled using the equation suggested by Mander et al. (1988) as

$$\sigma_c = \frac{f_c^{'}\lambda\left(\varepsilon_c/\varepsilon_c^{'}\right)}{\lambda - 1 + \left(\varepsilon_c/\varepsilon_c^{'}\right)^{\lambda}} \tag{1}$$

where σ_c = the longitudinal compressive concrete stress; $f_c^{'}$ = the compressive cylinder strength of concrete; ε_c = the longitudinal compressive concrete strain; $\varepsilon_c^{'}$ = the strain at $f_c^{'}$. The parameter λ is defined by

$$\lambda = \frac{E_c}{E_c - \left(f_c^{'}/\varepsilon_c^{'}\right)} \tag{2}$$

where E_c = the Young's modulus of concrete. The strain $\varepsilon_c^{'}$ is taken as 0.002 for concrete strength under 28 MPa and 0.003 for concrete strength over 82 MPa. When the concrete strength is between 28 and 82 MPa, the strain $\varepsilon_c^{'}$ is determined as a linear function of the concrete strength.

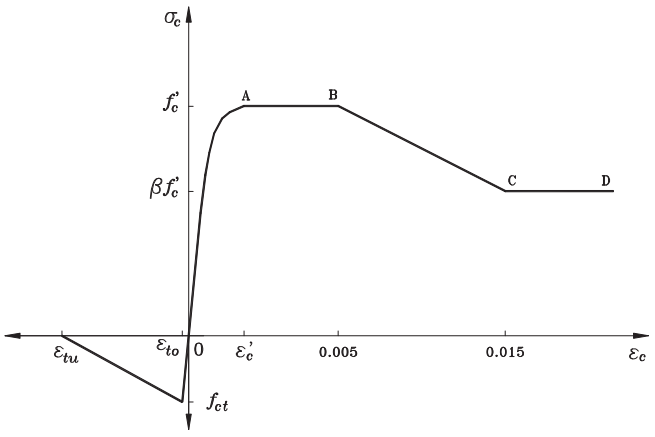

Figure 2. Stress-strain relationship for concrete in CFST columns

The parts AB, BC, CD of the stress-strain curve for confined concrete depicted in Figure 2 are defined as follows:

For $\varepsilon_c' < \varepsilon_c \le 0.005$,

$$\sigma_c = f_c' \tag{3}$$

For $0.005 < \varepsilon_c \le 0.015$,

$$\sigma_c = \beta f_c' + 100(0.015 - \varepsilon_c)(f_c' - \beta f_c') \tag{4}$$

For $\varepsilon_c > 0.015$,

$$\sigma_c = \beta f_c' \tag{5}$$

where β is taken as 1.0 when the width-to-thickness ratio (*B/t*) of the composite column is less than 24 and is taken as 0.0 when the *B/t* ratio is greater than 64 as suggested by Tomii and Sakino (1979). For *B/t* ratios between 24 and 64, β is taken as 0.6 in the fiber element analysis program.

The stress-strain relationship for concrete in tension as depicted in Figure 2 assumes that the tension stress increases linearly with an increase in tensile strain up to concrete cracking. After concrete cracking, the tensile stress decreases linearly to zero as the concrete softens. The tensile strength of concrete is taken as $0.6\sqrt{f_c'}$ while the ultimate tensile strain is taken as 10 times of the strain at cracking.

2.4 *Stress resultants*

Member forces are determined as the stress resultants in the composite section by

$$P = \sum_{i=1}^{ns} \sigma_{s,i} A_{s,i} + \sum_{j=1}^{nc} \sigma_{c,j} A_{c,j} \tag{6}$$

$$M_x = \sum_{i=1}^{ns} \sigma_{s,i} A_{s,i} y_i + \sum_{j=1}^{nc} \sigma_{c,j} A_{c,j} y_j \tag{7}$$

$$M_y = \sum_{i=1}^{ns} \sigma_{s,i} A_{s,i} x_i + \sum_{j=1}^{nc} \sigma_{c,j} A_{c,j} x_j \tag{8}$$

where P = the axial force; M_x = bending moment about the major principal axis; M_y = bending moment about the minor principal axis; $\sigma_{s,i}$ = the longitudinal stress at the centroid of steel fiber *i*,; $A_{s,i}$ = the area of steel fiber *i*; $\sigma_{c,j}$ = longitudinal stress at the centroid of concrete fiber *j*; $A_{c,j}$ = the area of steel fiber *j*; x_i and y_i = the coordinates of steel fiber *i*; x_j and y_j = the coordinates of concrete fiber *j*; ns = the total number of steel fiber elements; and *nc* = the total number of concrete fiber elements. The origin of the coordinate system is at the centroid of the composite section as depicted in Figure 1. Compressive stresses are taken to be positive. The stresses in fibers are calculated using fiber strains and stress-strain relationships.

2.5 *Secant algorithms*

For composite sections under axial load and biaxial bending, strains in the sections are a function of the curvature (ϕ), neutral axis orientation (θ) and strain at the extreme fiber (ε_t). For a given axial load, the curvature is gradually increased and the depth and orientation of the neutral axis need to be adjusted to satisfy the equilibrium conditions. Although the bi-section method can be used to adjust the depth and orientation of the neutral axis in the nonlinear analysis of composite sections, its convergence is very slow. The quasi-Newton method within the Regular-Falsi numerical scheme has been employed to determine the depth and orientation of the neutral axis by Chen et al. (2001). In the present method, secant algorithms are developed and implemented in the fiber element analysis program to iterate the depth and orientation of the neutral axis until equilibrium conditions are satisfied. The neutral axis depth (d_n) is updated by

$$d_{n,\,j+2} = d_{n,\,j+1} - \frac{(d_{n,\,j+1} - d_{n,\,j}) f_{p,\,j+1}}{f_{p,\,j+1} - f_{p,\,j}} \tag{9}$$

where d_n = the neutral axis depth; the subscript j = the iteration number; and f_p is determined by

$$f_p = P_n - P \tag{10}$$

where P_n = the given axial load.

The orientation of the neutral axis with respect to the *x*-axis as shown in Figure 1 is updated by

$$\theta_{k+2} = \theta_{k+1} - \frac{(\theta_{k+1} - \theta_k) f_{m,k+1}}{f_{m,k+1} - f_{m,k}} \tag{11}$$

where θ = the angle of the neutral axis; the subscript k = the iteration number; and f_m is expressed by

$$f_m = Tan\alpha - M_y / M_x \tag{12}$$

where α = the angle of the applied load as depicted in Figure 1.

The secant algorithm needs two initial values to start the iteration process. In the present method, the initial values for the neutral axis orientation (θ_1, θ_2) are set to α and $\alpha/2$ respectively while the initial values of the neutral axis depth $(d_{n,1}, d_{n,2})$ are set to *D* and *D/2*.

2.6 *Solution procedure*

In the fiber element analysis of CFST beam-columns, the axial load is incrementally increased from zero to the maximum value $P_{\max}$. The maximum axial load $P_{\max}$ can be determined from the axial load-strain curve as presented by Liang et al. (2006). For each load increment applied at a fixed angle (α), the moment-curvature response can be obtained by incrementally increasing the curvature and solving for the corresponding moment value. The solution procedure is given as follows:

(1) Calculate the maximum axial load ($P_{\max}$) for the composite section and specify the load increments.
(2) Specify initial values for the eccentricity angle α and curvature ϕ.
(3) Initialize: $\theta_1 = \alpha; \theta_2 = \frac{\alpha}{2}; d_{n,1} = D; d_{n,2} = \frac{D}{2}$.
(4) Calculate f_p and f_m for the two initial values of the neutral axis depth and orientation.
(5) Calculate fiber strains and stresses and the resultant force *P*.
(6) Adjust the depth of the neutral axis d_n using Eq. (9).
(7) Repeat Steps (2) to (6) until $f_p < \varepsilon_k$.
(8) Calculate bending moments M_x and M_y.
(9) Adjust the orientation of the neutral axis (θ) using Eq. (10).
(10) Repeat Steps (2) to (9) until $f_m < \varepsilon_k$.
(11) Calculate the resultant bending moment $M = \sqrt{M_x^2 + M_y^2}$.
(12) Update $M_{\max}$ if $M > M_{\max}$.
(13) Increment the curvature until the maximum bending moment is obtained.
(14) Increment the axial load P_n.
(15) Repeat Steps (2) to (14) until the maximum axial load increment is reached.

In the above solution procedure, the convergence tolerance ε_k can be taken as 10^{-4} to 10^{-6}. In all analyses presented in this study, the tolerance of $\varepsilon_k = 10^{-4}$ was used.

3 COMPARISONS WITH EXISTING SOLUTIONS

To verify the fiber element analysis program developed, the axial load-bending moment interaction curve for a short CFST beam-column predicted by the present method is compared with those obtained by other researchers. A CFST column with a section of $150 \times 100 \times 5$ mm tested by Shakir-Khalil and Al-Rawdan (1996) was analyzed using the fiber element analysis program. The yield strength of the steel section was 350 MPa and the compressive concrete cube strength was 45 MPa. The *B/t* ratio of steel plates that formed the steel box was 30. The section of these steel plates with *B/t* = 30 was considered as compact and the effects of local buckling were neglected in the analysis (Laing et al. 2007). Figure 3 depicts the axial load-bending moment interaction curves generated by the fiber element analysis technique and provided by Shakir-Khalil and Al-Rawdan (1996) and Lakshmi and Shanmugam (2002). It can be seen from the figure that the interaction curve obtained by the fiber element analysis technique agrees very well with those given by other researchers. For axial load below 600 kN, the bending moment capacity predicted by the fiber element method was between those values given by Shakir-Khalil and Al-Rawdan and Lakshmi and Shanmugam. It appears that the results given by Lakshmi and Shanmugam were conservative because their model did not considered the tension strength of concrete.

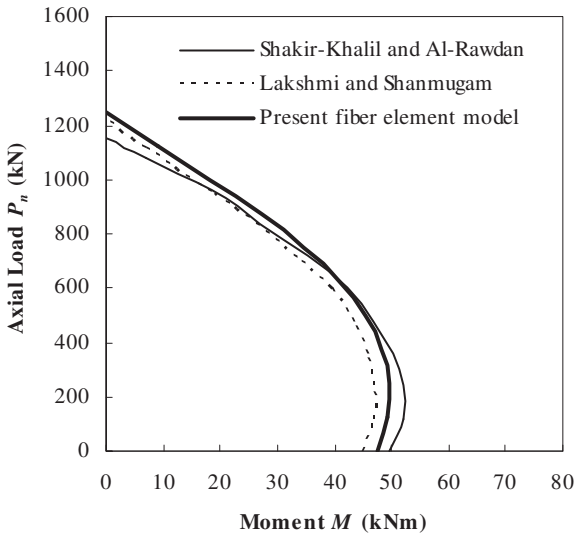

Figure 3. Comparison of axial load-bending moment interaction curves

4 STRENGTH INTERACTION CURVES

4.1 *Effects of steel ratios*

The effects of steel ratios on the axial load-bending moment interaction curves for CFST beam-columns under axial load and biaxial bending were investigated using the fiber element analysis program developed. The composite column section of 600×600 mm with structural steel ratios ($\gamma = A_s / A_g$) of 0.098, 0.129 and 0.19 were considered in the study. The angle of the applied load was fixed at 45^0. The steel yield strength was 300 MPa and the Young' modulus of steel was 200 GPa. The compressive cylinder strength of in-filled concrete was 28 MPa. The maximum compressive concrete strength was taken as $0.85f_c^{'}$ in the material model. The axial load-bending moment interaction curves for the CFST column section with various steel ratios are depicted in Figure 4, where P_o and M_o are the ultimate axial load and pure bending moment with a steel ratio of 0.098 respectively. The figure indicates that increasing the steel ratio in the composite section increased both the axial load and bending moment capacities. When the steel ratio in the composite section increased from 0.098 to 0.129 and 0.19, the axial load increased from $1.0P_o$ to $1.17P_o$ and $1.5P_o$ respectively and the pure bending moment capacity increased from $1.0M_o$ to $1.27M_o$ and $1.78M_o$, respectively.

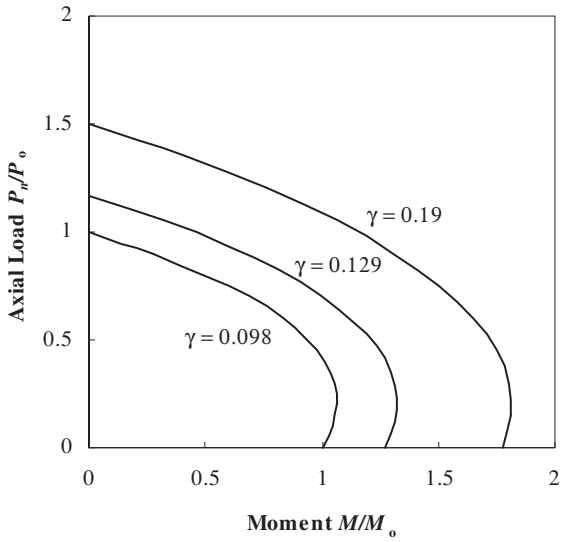

Figure 4. Effects of steel ratios on the axial load-bending moment interaction curves for CFST beam-columns

4.2 *Effects of concrete strengths*

The fiber element analysis program developed was employed to study the effects of concrete strengths on the axial load-bending moment interaction curves for CFST beam-columns under axial load and biaxial bending. The dimension of the composite section was 600×600 mm with a *B/t* ratio of 30. The steel box column was filled with 28, 69 and 110 MPa concrete respectively. The angle of the applied load was fixed at 45^0. The yield strength of the steel section was 300 MPa and the Young's modulus was 200 GPa. The maximum compressive strength of concrete was taken as $0.85f_c^{'}$ in the fiber element model.

Figure 5 depicts the axial load-bending moment interaction curves for the CFST beam-column filled with different strength concrete. It can be seen from the figure that increasing the concrete strength significantly increased the ultimate axial load while the pure bending moment capacity had a small increase. When the concrete strength increased from 28 to 69 and 110 MPa, the axial load increased from $1.0P_o$ to $1.5P_o$ and $2.0P_o$, and the pure bending moment capacity of the composite section increased from $1.0M_o$ to $1.09M_o$ and $1.15M_o$, respectively.

It can be concluded that the steel ratio in a composite section has a significant effect on the axial load and bending moment capacities of the composite section. Steel ratios in composite sections also improve the ductility of the sections as reported by Liang et al. (2006). However, the concrete strength has a significant effect on the axial load capacity of a composite section but not on its bending moment capacity.

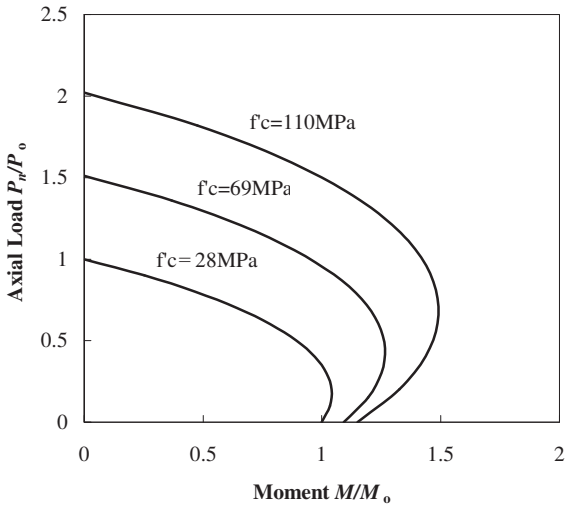

Figure 5. Effects of concrete strengths on the axial load-bending moment interaction curves for CFST beam-columns

5 CONCLUSIONS

A nonlinear fiber element analysis method has been presented in this paper for predicting the axial load-bending moment interaction curves for concrete-

filled steel tubular beam-columns under axial load and biaxial bending. Secant algorithms were developed and implemented in the fiber element analysis program to iterate the depth and orientation of the neutral axis in the composite column section to satisfy equilibrium conditions. The effects of steel ratios and concrete strengths on the axial-load bending moment interaction curves for CFST beam-columns were investigated using the fiber element analysis technique.

The secant algorithms and the fiber element analysis program developed were shown to be efficient for the nonlinear analysis of CFST beam-columns under axial load and biaxial bending. Parametric studies demonstrated that increasing the steel ratio in the section of a CFST beam-column increases both the axial load and bending moment capacities. The use of high strength concrete in CFST beam-columns results in a significant increase in the axial load capacities of the columns but only a small increase in the bending moment capacities. The proposed fiber element analysis technique can be used directly in the design of CFST beam-columns in practice.

6 REFERENCES

Bridge, R.Q, O'Shea, M.D., Gardner, P., Grigson, R. & Tyrell, J. 1995. Local buckling of square thin-walled steel tubes with concrete infill. In *Proceedings of the International Conference on Structural Stability and Design*, Sydney, Australia. 307-314.

Chen, S.F., Teng, J.G. & Chan, S.L. 2001. Design of biaxially loaded short composite columns of arbitrary section. *Journal of Structural Engineering*, ASCE 127(6): 678-685.

El-Tawil S., Sanz-Picón C.F & Deierlein G.G. 1995. Evaluation of ACI 318 and AISC (LRFD) strength provisions for composite beam-columns. *Journal of Constructional Steel Research* 34(1): 103-126.

El-Tawil S. & Deierlein, G.G. 1999. Strength and ductility of concrete encased composite columns. *Journal of Structural Engineering*, ASCE 125(9): 1009-1019.

Furlong, R.W. 1967. Strength of steel-encased concrete beam-columns. *Journal of Structural Division*, ASCE 93(5): 113-124.

Ge, H.B. & Usami, T. 1992. Strength of concrete-filled thin-walled steel box columns: experiments. *Journal of Structural Engineering*, ASCE 118(11): 3036-3054.

Hajjar, J.F. & Gourley, B.C. 1996. Representation of concrete-filled steel tube cross-section strength. *Journal of Structural Engineering*, ASCE 122(11): 1327-1336.

Knowles, R.B. & Park, R. 1969. Strength of concrete-filled steel tubular columns. *Journal of Structural Division*, ASCE 95(12): 2565-2587.

Lakshmi, B. & Shanmugam, N.E. 2002. Nonlinear analysis of in-filled steel-concrete composite columns. *Journal of Structural Engineering*, ASCE 128(7): 922-933.

Liang, Q.Q. & Uy, B. 2000. Theoretical study on the post-local buckling of steel plates in concrete-filled box columns. *Computers and Structures* 75(5): 479-490.

Liang, Q.Q., Uy, B. and Liew, J.Y.R. 2006. Nonlinear analysis of concrete-filled thin-walled steel box columns with local buckling effects. *Journal of Constructional Steel Research,* 62(6): 581-591.

Liang, Q.Q., Uy, B. & Liew, J.Y.R. 2007. Local buckling of steel plates in concrete-filled thin-walled steel tubular beam-columns. *Journal of Constructional Steel Research,* 63(3): 396-405.

Liang, Q.Q., Uy, B., Wright, H.D. & Bradford, M.A. 2004. Local buckling of steel plates in double skin composite panels under biaxial compression and shear. *Journal of Structural Engineering*, ASCE 130(3): 443-451.

Mander, J.B., Priestly, M.N.J. & Park, R. 1988. Theoretical stress-strain model for confined concrete. *Journal of Structural Engineering*, ASCE 114(8): 1804-1826.

Mursi, M. & Uy, B. 2003. Strength of concrete filled steel box columns incorporating interaction buckling. *Journal of Structural Engineering*, ASCE 129(5): 626-638.

Schneider, S.P. 1998. Axially loaded concrete-filled steel tubes. *Journal of Structural Engineering*, ASCE 124(10): 1125-1138.

Shakir-Khalil, H. & Al-Rawdan, A. 1996. Experimental behaviour and numerical modelling of concrete-filled rectangular hollow section tubular columns. In Dale Buckner, C. & Shahrooz, B.M. (ed.), *Composite Construction in Steel and Concrete III*, *Proceedings of an Engineering Foundation Conference*, Irsee, Germany, June 9-14, 222-235.

Shakir-Khalil, H. & Mouli, M. 1990. Further tests on concrete-filled rectangular hollow-section columns. *The Structural Engineer* 68(20): 405-413.

Spacone E. & El-Tawil, S. 2004. Nonlinear analysis of steel-concrete composite structures: state of the art. *Journal of Structural Engineering*, ASCE 130(2): 159-168.

Tomii, M. & Sakino, K. 1979. Elastic-plastic behavior of concrete filled square steel tubular beam-columns. *Trans. Arch. Inst*. Japan 280: 111-120.

Uy, B. 1998. Local and post-local buckling of concrete filled steel welded box columns. *Journal of Constructional Steel Research* 47(1-2): 47-72.

Uy. B. 2000. Strength of concrete-filled steel box columns incorporating local buckling. *Journal of Structural Engineering*, ASCE 126(3): 341-352.

Wright, H.D. 1995. Local stability of filled and encased steel sections. *Journal of Structural Engineering*, ASCE 121(10): 1382-1388,